Journal of Membrane Science and Research 5 (2019) 178-186

Journal of Membrane Science & Research

journal homepage: www.msrjournal.com

Research Paper

Advanced Dynamic Simulation of Membrane Desalination Modules Accounting for Organic Fouling

Anastasios J. Karabelas [1,*], Margaritis Kostoglou [2,1], Chrysafenia P. Koutsou [1]

[1] *Chemical Process and Energy Resources Institute, Centre for Research and Technology – Hellas, Thermi, Thessaloniki, Greece*
[2] *Division of Chemical Technology, Department of Chemistry, Aristotle University of Thessaloniki, Greece*

Article info

Received 2018-09-21
Revised 2019-01-07
Accepted 2019-01-08
Available online 2019-01-08

Keywords

Desalination
Reverse osmosis
Spiral wound membranes
Mathematical modeling
Organic fouling
Dynamic simulation

Highlights

- Development of a generalized framework for desalination membrane operation modeling
- Application of the advanced modeling framework for the case of organic fouling
- Submodels for deposit growth and its effect on all process parameters are included
- Computational results for typical conditions demonstrate the model/simulator capabilities

Graphical abstract

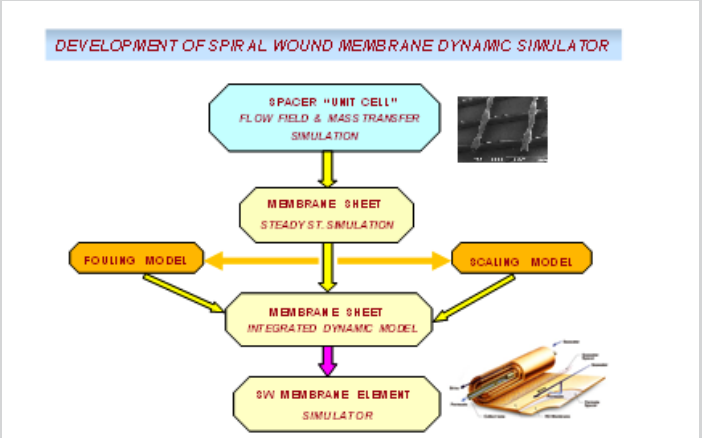

Abstract

A reliable dynamic simulator (based on a sound process model) is highly desirable for optimizing the performance of individual membrane modules and of entire desalination plants. This paper reports on progress toward development of a comprehensive model of the complicated physical-chemical processes occurring in spiral wound membrane (SWM) modules, that accounts for the temporal system variability caused by organic membrane fouling. To render the mathematical modeling-problem tractable, justified simplifications (retaining the physical parameter interdependencies) lead to a system of basic equations in two spatial planar coordinates, enabling to obtain a realistic temporal evolution of all process parameters at retentate and permeate flow channels of SWM modules. The developed flexible model structure, and process simulator, allow incorporation of sub-models (for phenomena occurring at small spatial scales during desalination) that account for a) feed-spacer effects on friction losses and mass transfer and b) membrane fouling. These sub-models, in the form of generalized expressions, are obtained for the former case through advanced numerical simulations, and for the latter by correlating experimental data of specific fouling resistance with permeation flux. Typical parametric study results presented herein, for realistic combinations of design and operating system parameters, demonstrate the versatility and reliability of the new model/simulator and its potential to analyze the complicated interaction of mechanisms involved during fouling evolution. The new results warrant further model development that would include other types of fouling and scaling, thus leading to a comprehensive simulator useful for practical applications.

1. Introduction

Ever-increasing R&D efforts are made to develop the membrane-desalination technology to the maximum extent possible, mainly aiming at reduction of product-water unit cost and mitigation of environmental impact [1, 2]. Achieving these targets depends on optimizing the design and operation of the desalination plant, which is comprised of pressure-vessel trains, each vessel containing several Spiral Wound Membrane (SWM) modules, as shown in Figure 1. Therefore, a reliable dynamic simulator (based on a sound process model), unavailable at present, is highly desirable for optimizing the detailed geometric characteristics and the performance of the individual SWM modules and of entire membrane plants [3, 4], for

* Corresponding author at: Phone: +30 2310- 498181, fax: +30 2310- 498189
E-mail address: karabaj@cperi.certh.gr (A.J. Karabelas)

DOI: 10.22079/JMSR.2019.94172.1216

various types of water treatment applications.

This study is focused on the SWM module, which is the key functional component of membrane desalination and water treatment plants [5], that are comprised of banks of pressure vessels [4, 5]. A cylindrical SWM element, shown in Figure 1, is made of several membrane "envelopes", each comprised of two membrane sheets with a permeate cloth/spacer in-between, glued at the three sides [5]. The envelopes are wrapped around a perforated permeate tube, and fixed along their fourth open side on this permeate tube. Thin net-type feed-spacers are placed in-between the envelopes, which form the retentate-side flow channels. With this design, modeling and simulating the performance of a single pressure vessel is sufficient for simulation of the entire desalination plant operation. Due to the filtration of permeate, the process conditions (trans-membrane pressure, permeation flux, velocities, etc.) significantly vary throughout the individual membrane envelopes comprising the SWM elements [6] as well as along the pressure vessel. Key feature of the compact design of SWM modules is the very narrow spacer-filled channel between envelopes (of gap less than 1mm), which aggravate operating problems; i.e. friction losses, membrane fouling and scaling [4, 5]. The compact design and the complicated flow field created by the spacers also hinder experimental and theoretical efforts aiming to investigate in detail SWM module performance. These difficulties have significant negative consequences in the development of models and simulation tools needed in the design and operation of RO process equipment and plants [4].

In addition to the inherent *spatial variability* of all process parameters under steady-state conditions (due to filtration) [6], membrane fouling leads to *temporal variability* of desalination module and plant operation [3]. Organic fouling is one of the most common problems of RO plant operation, significantly degrading SWM element performance, leading to increased energy consumption, deterioration of permeate quality and of overall process efficiency [7, 8]. The uneven development of fouling layers on RO membrane sheets is determined by the aforementioned locally varying process parameters; this spatial variability is clearly shown in recent studies [9, 10]. To improve SWM element design and operation, adequate knowledge is necessary on the spatial *and temporal* variation of the process parameters throughout the pressure vessels. Therefore, a reliable *dynamic simulator* is needed of SWM module performance, based on theoretically sound process modeling.

Some significant efforts have been reported on the development of *steady state* models, but not dynamic ones, as outlined in the following. Ghobeity and Mitsos [11] and Williams et al. [12] analyzed an interesting optimization problem of reverse osmosis plant operation; i.e. considering that the electricity price varies during a day (in accordance with the load on the electricity grid), they sought the optimum RO plant operation strategy during a day that would minimize the electricity/operating cost. A simple quasi-steady state model of the RO process was employed, considering that the flow rate and feed pressure are dynamic optimization variables. The problem was solved using advanced optimization techniques. Johannink et al. [13] presented an interesting generalized procedure for computing the two coefficients appearing in the friction factor-Reynolds number expression for spacer-filled channel flow. Instead of making CFD calculations for a specific spacer design and several Reynold numbers, several spacer designs were quantified through a large number of parameters. The complete space of parameter values could not be dealt with for such a large number of parameters; thus, a design of experiments (DOE) approach was taken to minimize the number of required simulations. Such simulations were performed for a membrane section that included 6 unit cells along the main flow and two unit cell across the main flow. Standard inflow and outflow conditions were employed with no accounting for periodicity in the flow direction. The Lattice Boltzmann method was employed to solve the governing equations, instead of the more common finite volume (or element) methods. Final result of this work [13] is generalized algebraic relations for the friction factor of non-woven and woven spacers for an extensive structural parameter space. Roy et al. [14] presented a fairly comprehensive model for nanofiltration modules, focusing on the effects of charge, pore radius and other membrane characteristics. A comparison was made between the results for the cases of flat-sheet and spiral-wound module configurations and useful insights were obtained. Despite the merits of the above studies [11-14], the respective models cannot be readily extended to account for temporal variability due to fouling. Hoek et al. [7] presented a semi-empirical model accounting for fouling in full-scale RO processes. This one-dimensional model considered local pressures, flows and concentrations, including the effects of concentration polarization and of resistance to permeation due to membrane fouling; the latter was assumed to be caused by a "cake" formation and (internal) membrane compaction. Key features of this model included: a) mass and momentum balances for the local transport, separation, and fouling processes; b) several fitting parameters that describe membrane, module, and foulant properties; and c) empirical correlations for mass transfer and hydraulic losses. Model performance was demonstrated by employing input data from a pilot-scale RO system and provided realistic results.

Authors of this paper have presented a comprehensive framework for modeling the performance of RO desalination SWM modules and pressure vessels [6, 15]. Detailed parametric studies for *steady state* desalination of brackish- and sea-water were performed, under constant pressure [9] and constant recovery [10] mode of operation, using a simulator based on the model. These studies showed the simulator capabilities that include the optimization of SWM module and spacer characteristics. The above model was later extended to address the dynamic simulation of SWM module performance under conditions of fouling [3].

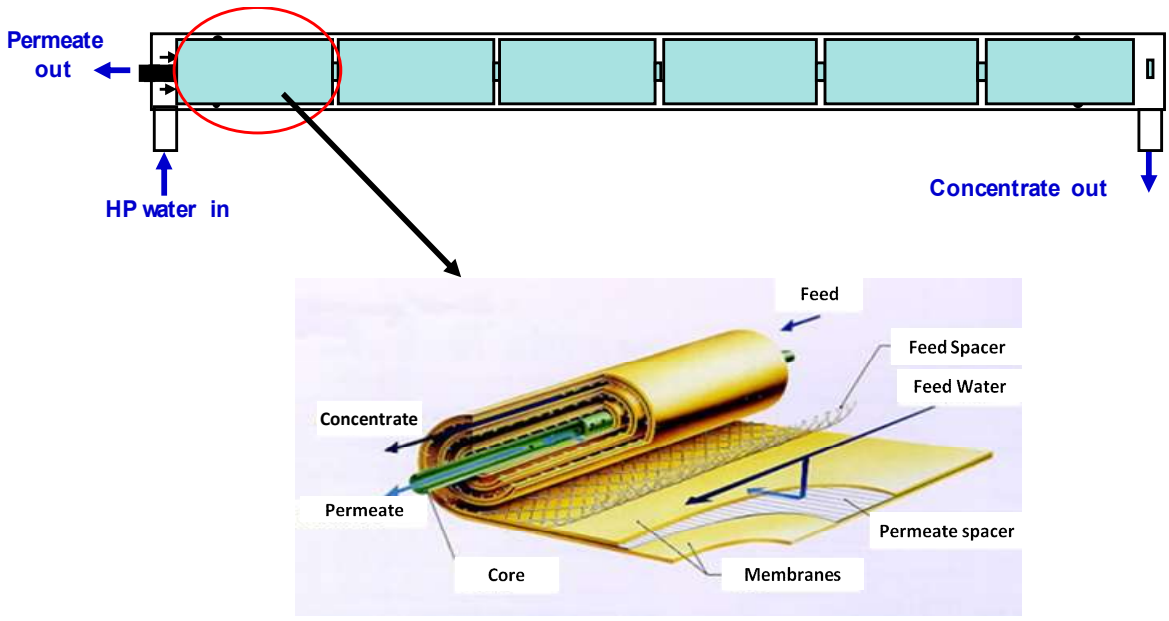

Fig. 1. A schematic of pressure vessel including several SWM modules, and a view of a SWM module indicating its function.

In parallel, correlations of a representative membrane-fouling parameter (i.e. the specific fouling resistance) were obtained for organic fouling of RO membranes, based on detailed laboratory studies [16, 17]. These correlations (akin to constitutive expressions) can serve as the necessary input to the dynamic simulator under development. Therefore, the present paper mainly aims : a) to outline the comprehensive mathematical model (and the respective simulator) of organic fouling evolution on the membrane sheets of SWM modules within a pressure vessel, operating under constant recovery, where account is taken of the spatial non-uniformities of the flow and concentration fields and their impact on the evolving deposit; b) to present typical results regarding the effect of main design and operating parameters on fouling evolution throughout the membrane sheets of SWM modules, along a pressure vessel; c) to outline R&D priorities toward further development of the dynamic simulator.

2. Mathematical modeling

Mathematical modeling of the dynamic operation of a membrane element undergoing organic fouling is a difficult task due to the complexity of the underlying physical and chemical processes and of the complicated channel geometry [3]. The problem is of multiscale nature since it includes spatial scales extending from the micro-scale of the fouling layer development to the large scales of the whole SWM element and of the multi-element pressure vessel. The starting geometry for the model development is the planar membrane sheet and the problem definition domain is half a retentate and half a permeate channel with the membrane in-between [4, 6], as shown in Figure A1 (Appendix). The formulation of the retentate side problem is based on the Navier-Stokes equations that must be solved in the liquid domain which is defined from the spacers and the membrane/channel walls. Regarding the formulation of permeate side, flow in porous media is considered since the void size is much smaller than the channel width so that the homogenization procedure can be applied. The two flow fields are connected through the Darcy law integrated across the membrane that separates the two channels. The formal boundary conditions are the inlet/feed pressure, retentate outlet and permeate outlet pressures. The pressure difference between inlet and permeate outlet drives the separation process, whereas the difference between inlet and retentate outlet pressure drives the retentate flow. The practical boundary conditions are inlet and permeate pressures and total flow rate. The aforementioned equations constitute the purely hydrodynamic problem [6].

There is a two way coupling between the flow and concentration fields. The concentration depends on velocity through the convection terms and the velocity depends on concentration through the osmotic pressure which determines the wall flux. Typically, the rejection of the ionic species is incomplete, thus a small amount can pass to the permeate channel. This phenomenon is described through the so called rejection coefficient R which is a local characteristic of the membrane and it is related to the membrane properties (pore size distribution, charges) through lower scale theories. Therefore, the conservation equation must be also solved in the permeate side for the incompletely rejected ionic species. Conservation equations must be also considered for the organic foulants, which undergo complete rejection by RO membranes. The previous discussion refers to the absence of any type of material accumulation in the membrane element. Material accumulation can occur by flux-induced deposition on the membrane of organic substances dissolved in the water. A gel layer is commonly created from organic macromolecules transferred with the flow on the membrane [16, 17]. The properties of this fouling layer depend on the local trans-membrane pressure and the instantaneous permeation flux [16], and (in turn) they affect the local flow conditions as well as the flux due to the added resistance to permeation.

The disparate size scales of the problem make a direct attack of the point-wise conservation equations computationally intractable; therefore, a scale decomposition approach is followed [4]. The governing equations of this modeling approach are outlined in the Appendix**.** The equations are integrated across the normal (to the membrane and main flow) direction and they are homogenized at the scale of the spacer unit cell [4, 6]. The closure is achieved through constitutive-type expressions for pressure drop and mass transfer in the spacer-filled channels. These expressions are derived through Computational Fluid Dynamic simulations at the unit cell scale [18, 19]. A typical mesoscale *clean membrane model* consists of the solvent and solute conservation equations in retentate and permeate sides, equations for pressure in both sides, of the membrane transport model and of a relation between the average bulk (cup-mixing) solute concentration and its concentration on/at the membrane (Eqs. A2 – A6). The difference between these two concentrations is due to the so-called *concentration polarization* phenomenon (Eq. A7). The communication between the spacers scale and mesoscale is through relations for the friction factor and mass transfer in the retentate channel (Eq. A1 and A8) [18, 19]. The former is used in mesoscale for pressure drop evaluation and the latter to account for concentration polarization. The effect of foulant layer is to reduce the local membrane permeability as well as the local mass transfer coefficient (cake-enhanced concentration polarization) [20]. Both phenomena are taken into account by using appropriate constitutive expressions for organic fouling (Eqs A9 – A11) developed in this laboratory [16] and an effective diffusivity through the fouling layer D_e (Eq. A8) [17]. The local rejection coefficient is related to the local wall flux and solute concentration through the Spiegler-Kedem model [21].

The final problem to be solved consists of a set of non-linear partial differential equations in two spatial and one temporal coordinate [3]. The solution algorithm employed is very robust and unconditionally stable. The particular normalization of equations used, allows a relatively small number of discretization steps, because only steps with essential variable advancement are implemented. The system of equations is solved using an iterative (Gauss-Seidel) scheme. Non-linear closure algebraic relations are solved for each spatial position by combining a bisection and Newton-Raphson method. The starting values for iteration are crucial for the stability of the algorithm; thus, an approximate analytical prediction for retentate outlet pressure is used as starting value. The situation is more complicated in the constant flux case, where the secant method is used at each time step to determine the inlet pressure that leads to the required flux.

3. Results and discussion

In recent studies, the steady state model of Kostoglou and Karabelas [6] was employed for simulating the performance of a 7-element pressure vessel under constant pressure [9] and constant recovery [10]. This model takes into account the interaction of the aforementioned operating and design parameters which affect the SWM element performance. The computational results include macroscopic/averaged parameters (i.e. SWM permeate productivity, feed pressure, pressure drop, etc.) as well as spatial distribution of all system parameters including local trans-membrane pressure, permeate and retentate velocities, permeate flux, bulk and wall concentrations. From these parametric studies, a combination of SWM geometric parameter values emerges (called “best” case) which leads to improved, near optimum, module performance.

Essentially the same two sets of SWM geometric design parameters of the steady-state operation (designated as “reference” and “best” case [9, 10]) are employed in this presentation. In particular, this work deals with the effect of a growing organic fouling layer on the spatial and temporal evolution of process parameters for a pressure vessel that includes four (4) SWM modules and operates under typical *constant recovery* conditions. Brackish water desalination is considered in this work. Relevant organic fouling layer properties are presented in [16, 17]. Operating and geometric parameter values of the present simulations are listed in Table 1; the same values, typical of those encountered in practical applications, were employed in previous steady-state simulations of brackish-water desalination under *constant feed pressure* [9] and *constant recovery* [10] mode of operation.

Indicative simulation results are provided to demonstrate the potentialities of the novel dynamic simulator for brackish-water RO desalination. It should be emphasized that the calculations are representative of the initial phase of growing organic deposits (starting from a clean membrane), where relatively thin fouling layers are involved; moreover, the simulations (for the entire pressure vessel) are carried out in time steps until a mean fouling layer thickness develops which is equal to 10% of the diameter of the feed-spacer cylindrical filament on each membrane of the feed channel. Therefore, this value corresponds to 10% reduction of the retentate channel gap h_r; i.e. $0.1h_r$. To facilitate the presentation, time intervals equivalent to equally-spaced fouling thickness fractions are employed; i.e. $0.01h_r$, $0.02h_r$, $0.03h_r$, etc., which are referred to as 1st, 2nd, 3rd, etc. time interval, respectively.

Figure 2 shows the variation of mean permeate flux (per SWM element) along a 4-element pressure vessel, subject to organic fouling, under conditions listed in Table 1. It is noteworthy that, under the imposed constant recovery 45%, there is essentially no effect of fouling on these global average (per element) fluxes even though the spatial distribution of fouling layer thickness and of other important operating parameters significantly change with time, as subsequently shown.

It will be also observed that the axial variation of the mean flux per SWM element of the 4-element vessel examined here is very close to that of a 7-element pressure vessel operating at steady-steady with 70% recovery [10]. Figure 3 depicts the temporal evolution of the space-averaged fouling layer thickness, per SWM element, for test conditions of the “reference case” (see Table 1). As one would expect, on the basis of intuition as well as observations and autopsies of real SWM modules (e.g. [22]), the fouling layer thickness tends to increase more in the leading elements, where the fluxes are greater.

Table 1
SWM module design and operating parameters for brackish water treatment.

Feed Water Characteristics		
Salinity (NaCl concentration)	2000 mg/L	
Foulant (alginate) concentration	2 mg/L	
Diffusivity within gel fouling layer [17]	$1.44x10^{-9}$ m^2/s	
Specific Cake Resistance [16], $a=\gamma J^{\beta}$	$\gamma = 6 \cdot 10^{20}$ s/kg, $\beta=1$	
Operating Parameters		
Feed Flow Rate, Q	9.84 m^3/h	
Recovery, R	45%	
SWM Module Design Parameters		
Membrane Resistance, R_m	Reference Case	Best Case
	$0.9x10^{14}$ m^{-1}	$0.9x10^{14}$ m^{-1}
Membrane Area, A	$38.5m^2$	
Number of Envelopes, N	15	30
Membrane Sheet Length, L	1 m	
Membrane Sheet Width, W	1.284 m	0.642 m
Retentate Spacer Geometry	L/D=8, β=90°	L/D=12, β=105°
Retentate Channel Gap, h_r	0.71 mm (28 mil)	0.86 mm (34 mil)
Permeate Channel Gap, h_p	0.23 mm	
Permeate Spacer Lateral Permeability, k	$2.0x10^{-10}$ m^2	$5.0x10^{-10}$ m^2

The strong effect of increasing fouling layer thickness (Figure 3) on the element pressure drop and feed pressure are shown in Figures 4 and 5, respectively. The SWM element pressure drop (see Figure 4) tends to increase with time, as expected. This increase is more evident in the leading elements where higher velocities prevail in the retentate channels; i.e. the increasing fouling layer thickness causes increased local velocities and pressure drop in the leading elements. Additionally, it is observed that the pressure drop for the "best" case is significantly smaller, compared with the "reference" one; this is caused by the smaller feed flow velocities (for the same feed flow rate) due to the greater channel gap (34mil for the best case and 28mil for the reference one). Figure 5 exhibits the temporal evolution of the feed pressure for each element of the pressure vessel, where it is evident that the best case requires a significantly smaller level of feed-pressure. However, it should be noted that the rate of increase of feed pressure for the "best" case is somewhat greater compared to that of the "reference" case. This interesting trend may be the net outcome (on channel gap and pressure drop) of the different spatial distribution of foulants in the two cases, even though the spatially averaged thicknesses per SWM element are nearly the same. These effects deserve additional attention in future studies.

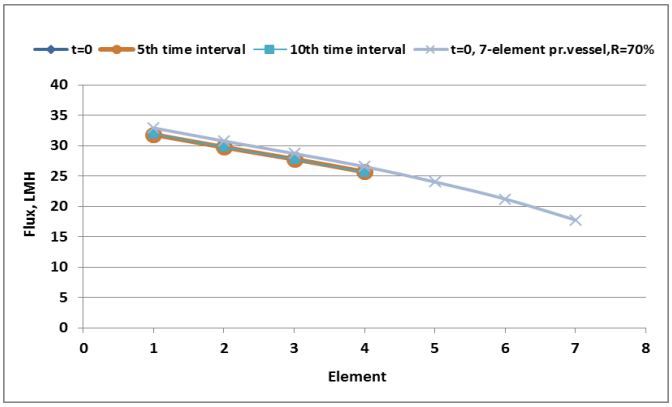

Fig. 2. Brackish water desalination. Variation of mean permeate flux along a 7-element pressure vessel, operating at steady-state with 70% recovery, compared to similar variation of a 4-element pressure vessel (using the same SWM element type) subject to fouling, at constant recovery 45%. : Parameters for "reference case".

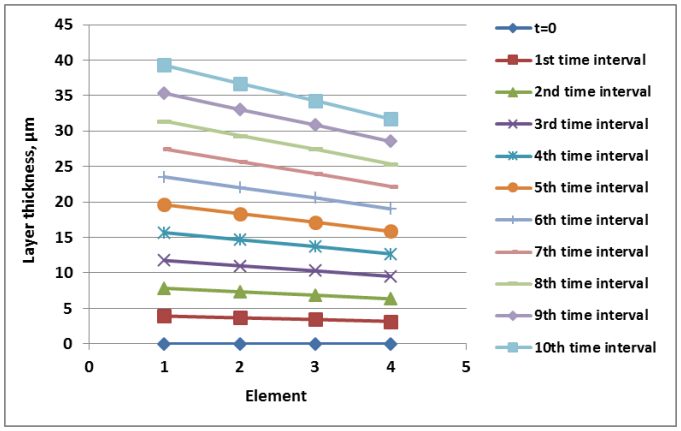

Fig. 3. Temporal evolution of the *space-averaged* fouling layer thickness, per SWM element, for the set of geometric parameters corresponding to the "reference case".

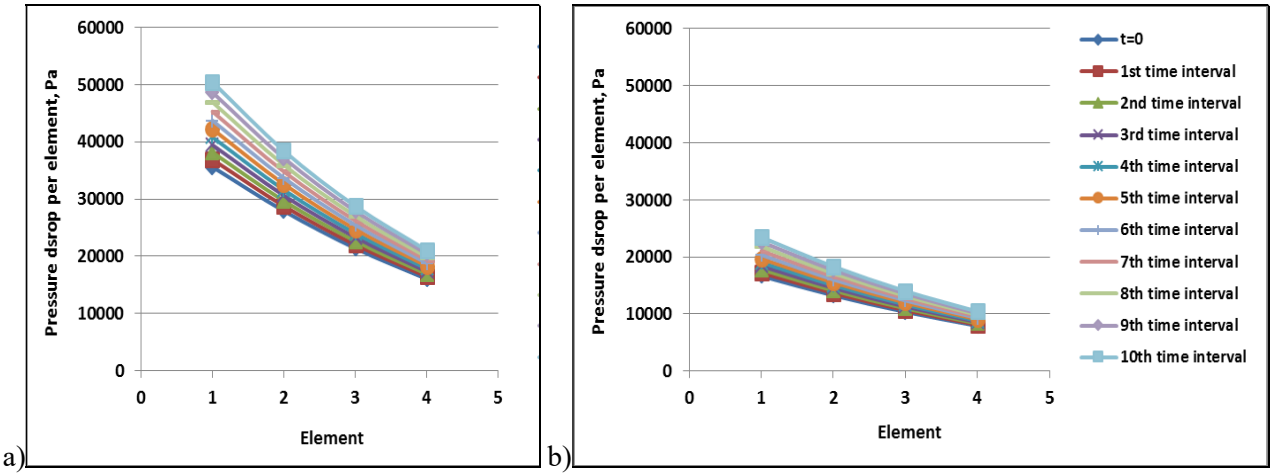

Fig. 4. Temporal evolution of pressure drop in each SWM element, along the pressure vessel, for the set of geometric parameters corresponding to a) Reference Case and b) Best Case.

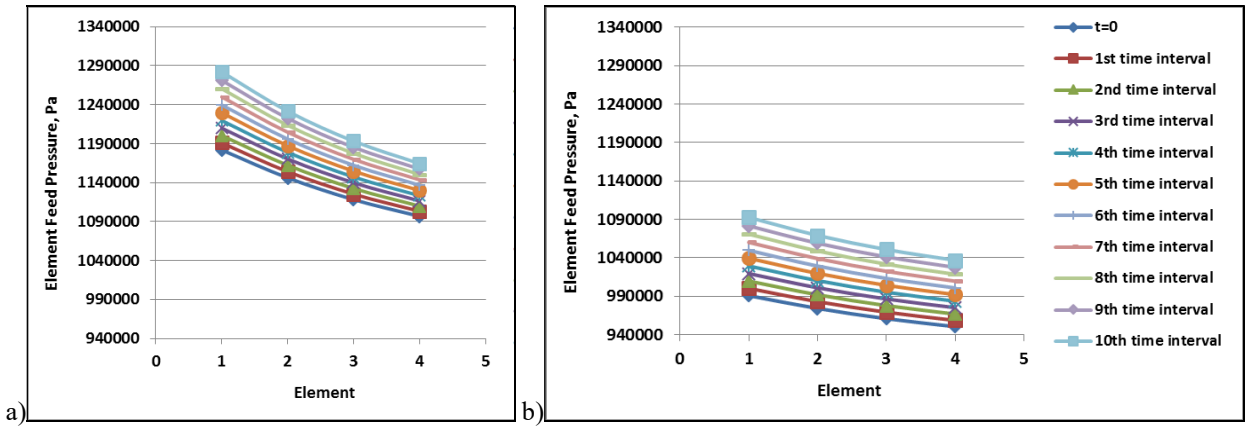

Fig. 5. Temporal evolution of feed pressure to each SWM element, along the pressure vessel, for the set of geometric parameters corresponding to a) Reference Case and b) Best Case.

The negative effect of fouling layer development on the salt rejection and the quality of permeate is clearly shown in Figure 6**,** for the two types of SWM modules considered in this study. Under steady-state conditions (t=0), one observes the well-known axial increase of salts concentration due to the increasing retentate membrane surface concentration C_w, shown in Figure 6. With the increasing fouling layer thickness, the systematic increase of local C_w (see Figure 6) apparently leads to degrading salt rejection and to increased permeate concentration.

Figure 7 presents snap-shots indicative of the temporal evolution of the fouling layer-thickness spatial distribution, throughout the four SWM elements of the pressure vessel, and for the geometric parameter set corresponding to the "reference" case. Starting from a clean membrane, initially the fouling layer thickness seems to exhibit spatial uniformity; however, as the time progresses the organic foulants tend to deposit unevenly on the membranes, especially in the leading SWM elements. In fact, the greater values of fouling layer thickness are observed close to the permeate tube (in the leading SWM element) where the greater permeation fluxes are encountered. This trend is expected, as it is caused by the correspondingly uneven spatial distributions of the trans-membrane pressure (TMP) shown in Figure 8. Indeed, the greater local TMP values near the permeate collection tube are associated with greater local fluxes (predicted by the well-known Darcy expression), as discussed in detail elsewhere [9, 10]; in turn, the increased local fluxes cause increased foulants deposition and resistance to permeation, as shown and quantified for depositing organic gels elsewhere [4, 16].

It is interesting to note that the interacting mechanisms (membrane rejection and/or permeation of various species, organic matter deposition on membranes, etc.) leading to evolution and spatial (re-)distribution of key variables (i.e. TMP, permeate flux, foulant thickness) is quite complicated and can be resolved only by the type of comprehensive modeling and simulation presented here; i.e. space averaged quantities are not helpful in this respect. For instance, one would intuitively expect a kind of *"smoothing effect"* of these fouling phenomena in the case of *constant mean recovery* operation. Specifically, the fouling layer thickness and resistance to permeation would tend to increase in some regions of the membrane sheet (e.g. close to the permeate tube) where the TMP is greater, as shown in Figure 8. However, the local flux there would tend to be reduced, whereas in other regions of the membrane, initially characterized by smaller thickness and specific resistance, the flux would tend to increase somewhat, so that a constant overall permeate recovery would be maintained. In turn, the rate of foulant deposition in the latter regions would tend to increase somewhat due to this local flux increase, thus leading to a kind of spatial "smoothing" of the fouling layer thickness. The data in Figure 6, appear to display this trend; indeed, despite the significant growth of *the mean* fouling layer thickness with time, there are relatively modest differences in the thickness spatial distributions among the various SWM modules. Similarly, as shown in Figure 8, despite the significant increase of feed-pressure and of the *mean* TMP, the local TMP distributions in each SWM module tend to maintain their form, with modest change.

It is noted that predictions of a semi-empirical model developed by Hoek et al. [7], fitted to a RO pilot system operation, suggest that a so-called "flux leveling" induced by fouling may occur, whereby fluxes at the rear SWM modules would tend to increase with time, while those at the front would decrease, for constant recovery. These predictions are in line (at least qualitatively) with the aforementioned fouling layer "smoothing effect" and partial redistribution of the various system parameters (local fluxes, TMP, etc.), demonstrated by these simulations. It should be added that in SWM modules with smaller width of membrane-sheets, the smoothing effect would lead to more even distributions (throughout a sheet) of all system parameter.

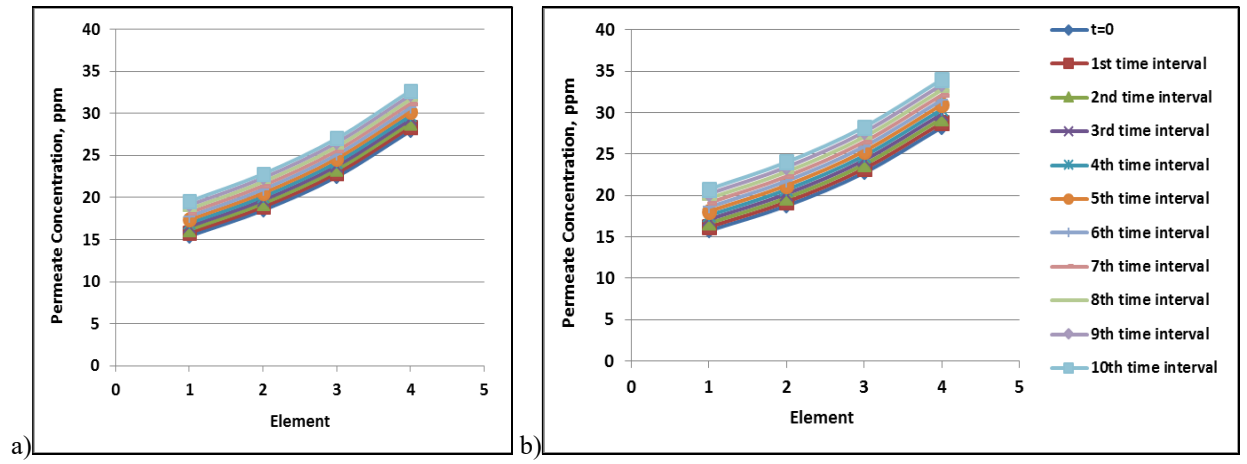

Fig. 6. Temporal evolution of *mean permeate concentration* exiting each SWM element, along the pressure vessel, for the set of geometric parameters corresponding to a) Reference Case and b) Best Case.

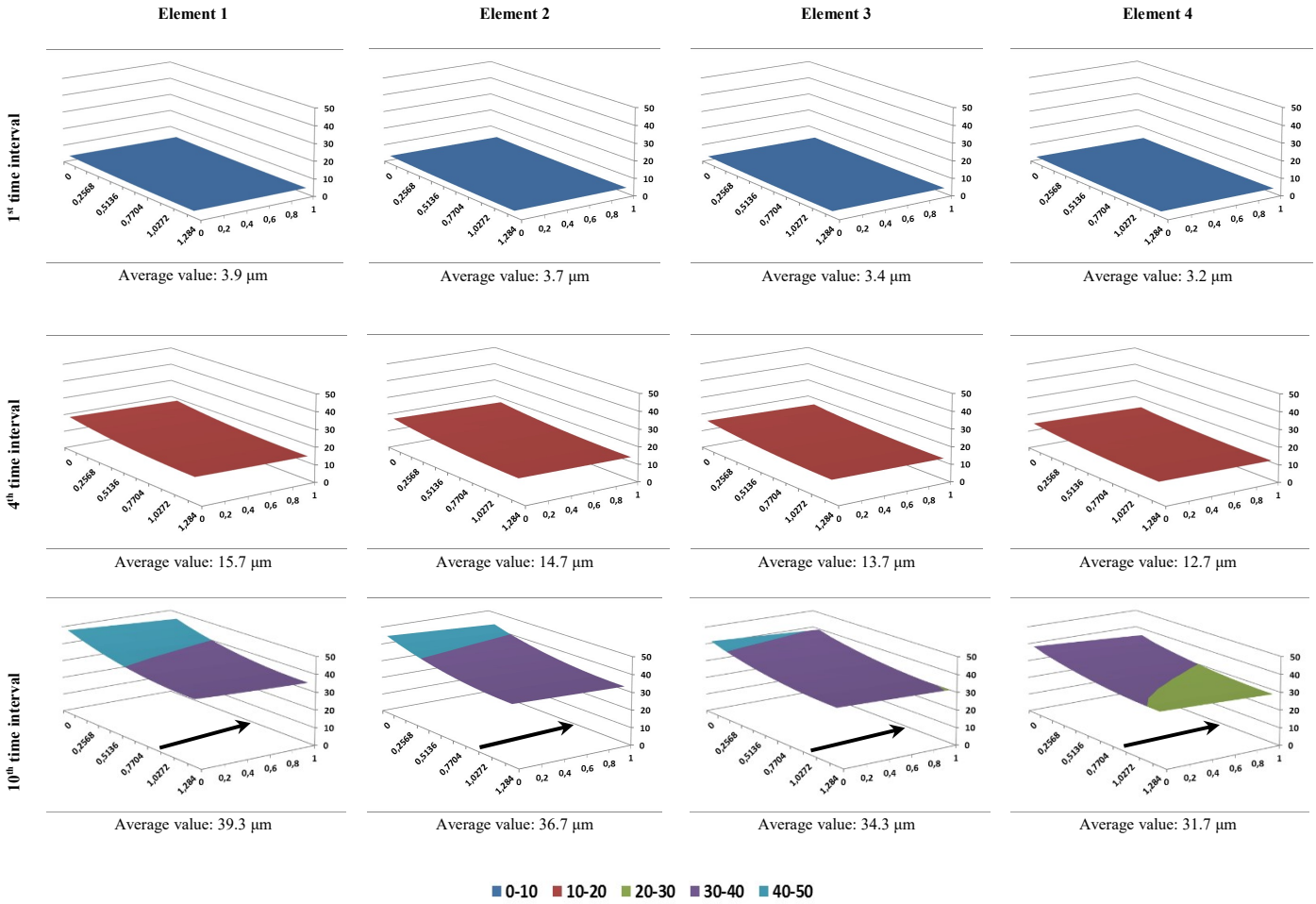

Fig. 7. *Brackish water desalination.* Typical spatial distributions of the fouling layer thickness (in μm), evolving in time, for the four SWM elements of the pressure vessel considered in this work. The conditions correspond to the "reference" case (Table 1). The arrows indicate the direction of main flow.

Of significant practical and theoretical interest is the spatial variation of salts concentration at the membrane surface $C_{w,}$ as shown in the model predictions depicted in Figure 9. The uneven C_w distribution in the lateral (y) direction, with increased concentration toward the permeate tube, is expected as a direct outcome of the respective uneven TMP (see Figure 8) and flux distribution. At steady-state (t=0), the trend of increasing C_w along the pressure vessel is due to the loss of permeate. However, the temporal increase of membrane surface concentration C_w, with increasing fouling layer thickness, is particularly interesting. Indeed, it appears that the fouling-enhanced concentration polarization [20] dominates in this complicated process, even though the increasing thickness h of fouling layer tends to reduce the free cross-section, thus leading to increased flow velocity and mass transfer coefficient, for constant feed rate.

In this paper, time intervals are used to present simulation results that correspond to specified thicknesses h of the fouling layer. However, using estimates of the effective fouling layer density ρ_{ef} (Appendix), obtained from small-scale experiments, these intervals/ thicknesses correspond to real time of pressure vessel operation, starting from a clean membrane. For the conditions of the present simulations listed in Table 1, also assuming total deposition of the foulant mass contained in the permeating desalinated water, the real time corresponding to the 10^{th} interval is approximately 25 h.

4. Conclusions

A dynamic model has been developed to predict the SWM module performance when organic fouling occurs during RO-membrane desalination. The simulator is based on a comprehensive model, comprising a system of partial differential equations, in two spatial coordinates and a temporal one, as well as algebraic equations. Transversely averaged (across the channel gap) quantities are considered in both retentate and permeate channels. Account is taken of the effect of growing membrane-fouling layer on the feed pressure, pressure drop and mass transfer rates in the retentate channel that affect all SWM module operating parameters, including spatial-temporal distributions of trans-membrane pressure, permeate flux, and membrane wall concentration C_w.

Indicative results are presented (under constant recovery) which demonstrate the versatility of the model regarding the detailed simulation of desalination under a concurrently evolving organic fouling layer, and highlight the negative effect of fouling on the main process parameters; the latter include the increased resistance to permeation (that leads to increased feed-pressure) and the enhanced concentration polarization (that causes degradation of permeate quality). Additionally, interesting phenomena of spatial "smoothing" of the evolving fouling layer thickness are demonstrated. In general, the results show that one can obtain useful insights into the various interacting mechanisms during evolution of fouling, which is impossible by the much simpler one-dimensional models.

The general methodology demonstrated herein involves a) accurate description of fouling phenomena occurring at small scale, through correlation of key parameters (akin to constitutive expressions) obtained by appropriate experiments and b) integration of these expressions into a generalized modeling framework. This approach can serve as the basis for developing a comprehensive dynamic model of SWM-module performance (accounting for all types of fouling), and further a multi-purpose reliable simulator of RO/NF pressure-vessel and plant performance for practical applications. Since the dynamic model takes into account the geometric and other parameters of SWM module (i.e. the membrane envelope dimensions, spacer characteristics, permeability, etc.), the respective comprehensive simulator would be a most valuable tool for optimizing the design and operation of RO modules and plants. To achieve this challenging goal, significant R&D activity lies ahead that may be prioritized as follows:

i) Development of accurate *constitutive expressions/correlations* that describe particular membrane fouling/scaling phenomena *locally* as a

function of the main RO process parameters. Representative parameters of the particular fouling phenomena considered should be selected. For the initial stages of organic fouling, it is suggested that the key parameters are the *specific fouling-layer (or cake) resistance α* correlated with the *permeation flux J*; additionally, the rate of foulant mass deposition, and/or the fouling-layer thickness should be estimated. For incipient scaling, and other types of fouling (e.g. biofouling), different representative parameters may be required. Significant small scale laboratory work is required, for the various types of fouling, to address these issues.

ii) A *comprehensive data-base* should be developed (with results from the above and other similar literature studies), including the aforementioned representative fouling parameters and their correlation, for typical ranges of RO-process design and operating variables. Such a data-base would be very helpful for establishing generalized correlations, for assessing the fouling propensity of feed-fluids, and for dynamic simulations of RO plant performance.

iii) The complicated cases of combined types of fouling (e.g. organic-fouling/scaling, organic-fouling/colloidal-particulate fouling, biofouling/scaling) need particular attention, for implementing the methodology recommended here.

There are ongoing efforts in the authors' laboratory on the above fronts.

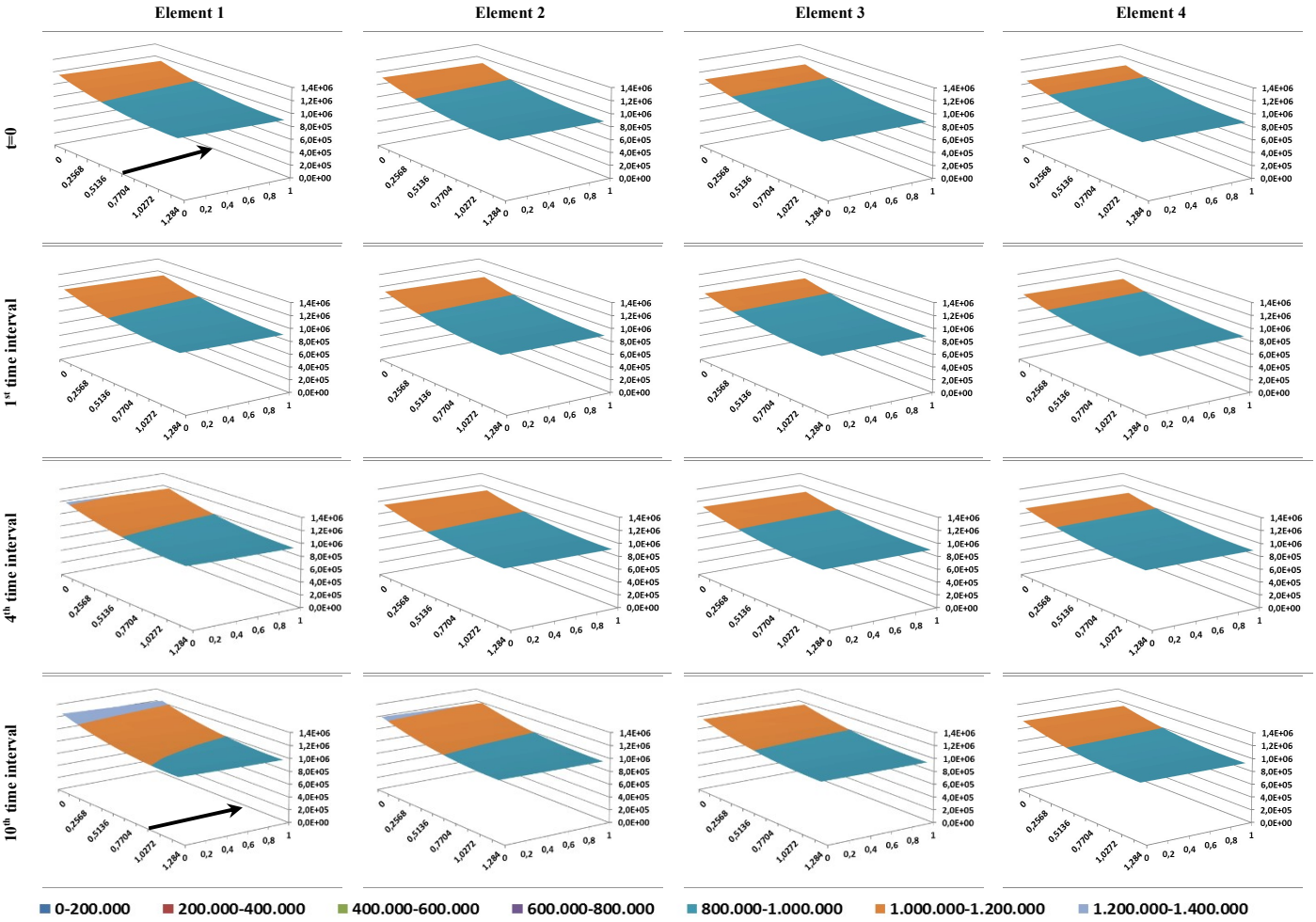

Fig. 8. *Brackish water desalination.* Temporal evolution of the spatial distributions of the trans-membrane pressure (TMP) (in Pa) for the four elements of the pressure vessel at constant recovery. Set of geometric parameter values corresponding to the "reference" case (Table 1).

Appendix

Governing equations of dynamic model

The governing equations of the model are presented herein. The planar coordinates along and across the membrane sheet (denoted as x,y) are common for both permeate and retentate channels. Thus, the length and width of the membrane sheet are L_x and L_y, whereas the gap of the permeate and retentate channel are L_{pz} and L_{rz} , respectively. The gap of the retentate channel is twice the spacer filament diameter D by construction (i.e. L_{rz}=2D). As the fouling layer grows to thickness h, the "open" half of the retentate channel is (D-h).

The fluid velocity in the retentate channel is related to the pressure drop as follows:

$$\vec{U} = -\left(\frac{(D-h)^{1+f_2}}{f_1 \rho^{1-f_2} \mu^{f_2}}\right)^{1/(2-f_2)} \left|\nabla p\right|^{(f_2-1)/(2-f_2)} \nabla p \qquad \text{(A1)}$$

where ρ, μ are the liquid density and viscosity respectively and f_1, f_2 are the parameters of the pressure drop-velocity relation for the particular spacer geometry considered.

The liquid mass balance in the *retentate channel* is described by the relation:

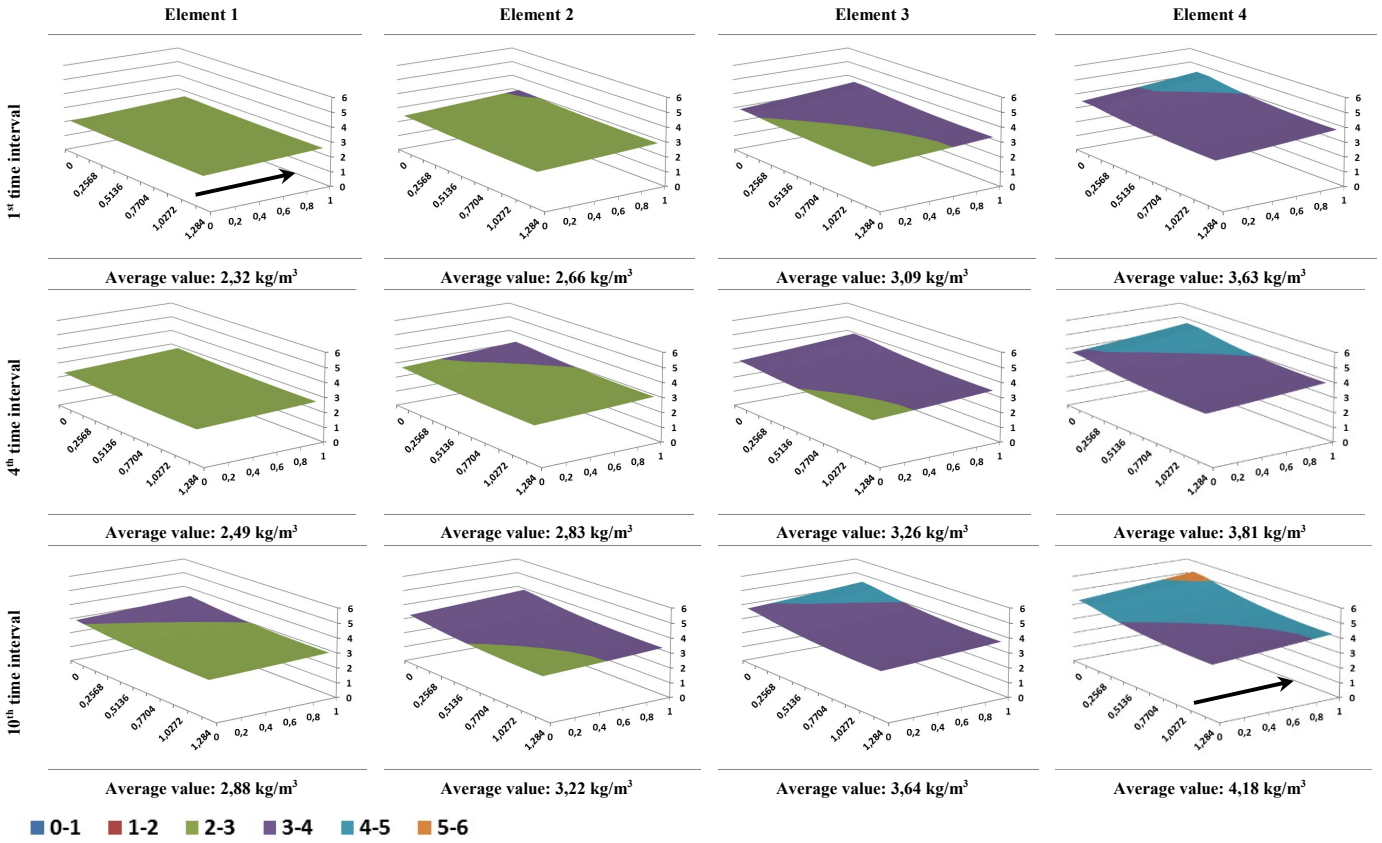

Fig. 9. Spatial-temporal evolution of *the local salt concentration*, throughout the membrane surfaces of each SWM element, along the vessel, for the set of geometric parameters corresponding to the Reference Case. Arrows indicate the retentate flow direction.

$$\nabla\cdot(\vec{U}(D-h))=-u_w \tag{A2}$$

where u_w is the wall velocity or permeate flux and $\vec{U}$ is the retentate velocity vector field having components U_x and U_y.

The pressure - velocity relation in the *permeate channel* is given as:

$$\vec{u}=-\frac{k}{\mu}\nabla P \tag{A3}$$

where k is the specific permeability of the permeate filler, $\vec{u}$ is the permeate velocity vector field with components u_x and u_y and P is the pressure at the permeate side.

The liquid mass balance in the permeate channel is given as:

$$\frac{1}{2}L_{pz}\nabla\cdot\vec{u}=u_w \tag{A4}$$

To describe the concentration field, the required variables are: the core (bulk) concentration in the retentate channel, C, the corresponding wall concentration, C_w, and the permeate channel concentration C_p.

The conservation equation for the core/retentate concentration is given as:

$$(D-h)\vec{U}\cdot\nabla C=u_w(C-(1-R)C_w) \tag{A5}$$

where R is the intrinsic rejection coefficient, i.e. a characteristic of the membrane considered. In general, R is a function of wall flux and local solute concentration and there are several models describing this dependence in the literature (e.g. [21]).

The conservation equation for the permeate-side solute concentration is as follows:

$$\frac{L_{pz}}{2}\vec{u}\cdot\nabla C_p=u_w((1-R)C_w-C_p) \tag{A6}$$

The wall solute concentration C_w is related to the local bulk concentration through the following relation, that accounts also for concentration polarization effects, e.g. [6].

$$C_w=C/(1-R+Re^{-u_w/k_m}) \tag{A7}$$

Here k_m is the mass transfer coefficient which is computed by the relation:

$$k_m=\left(\frac{h}{D_e}+\frac{D-h}{D_c g_1 Sc^{g_2} Re^{g_3}}\right)^{-1} \tag{A8}$$

where Sc is the Schmidt number, Re is the local channel Reynolds number (using D-h as characteristic length) and the dimensionless parameters g_1, g_2, g_3 depend on the type of the spacer geometry [18, 19]. The molecular diffusion coefficient of the foulant in the liquid is denoted as D_c whereas the effective diffusivity of the foulant in the fouling layer is denoted as D_e.

From the Darcy law, the following relation is obtained for the wall flux, that accounts for the developing fouling resistance:

$$u_w=\frac{p-P-\Gamma(C_w-C_p)}{\mu(R_m+\gamma u_w^{\beta}m)} \tag{A9}$$

where Γ is the so-called osmotic coefficient and R_m the clean membrane resistance. In Eq. (A9), the evolving fouling layer resistance R_c, is related to the permeate flux u_w and foulant depositing mass m (g/m^2) on the membrane,

as suggested by Karabelas and Sioutopoulos [16].

$$R_c = \alpha\, m = \gamma(u_w)^{\beta} m \qquad (A10)$$

Here α is the specific fouling layer resistance measured in appropriate tests (commonly at constant flux u_w) and correlated using the parameters γ, β.

The evolution of the fouling layer mass density m is given by the simple expression:

$$\frac{dm}{dt} = u_w C_f \qquad (A11)$$

where t is the filtration time (starting from a clean membrane) and C_f the concentration of the foulant assumed to be spatially uniform and equal to its inlet value. The fouling layer thickness h is related to the deposited foulant mass m through $h=m/\rho_{cf}$ where ρ_{cf} is the effective density of the layer (i.e. mass of organic material per unit volume of layer).

The physical boundary conditions are the inlet retentate pressure p_{in}, the outlet retentate pressure p_{out}, the zero retentate-channel velocity U_y at y=0 and $y=L_y$, the given inlet solute concentration C_o and the inlet foulant concentration C_f. The permeate channel boundary conditions are the reference pressure P=0 at y=0 and the zero normal velocity at $y=L_y$, x=0 and $x=L_x$. The mathematical problem is always solved using the above type of boundary conditions. The real system boundary conditions (prevailing during membrane operation), of a *fixed flow-rate and a fixed permeate recovery*, appear as integral constraints which must be satisfied by choosing appropriately p_{out} and p_{in} values. It is noted that in the general case the coefficients f_1,f_2, g_1,g_2,g_3 depend on the fouling layer thickness h. This dependence for a particular type of spacer can be found in [23].

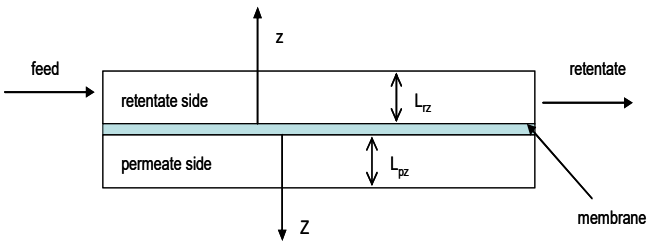

Fig. A1. Schematic cross-sectional view of the retentate and permeate flow channels. The retentate- and permeate-side spacers are not shown.

References

[1] A.J. Karabelas, C.P. Koutsou, D.C. Sioutopoulos, K.V. Plakas, M. Kostoglou, Desalination by Reverse Osmosis, in: Figoli A., Criscuoli A. (Eds.), Sustainable membrane technology for water and wastewater treatment, Green chemistry and sustainable technology, Springer, Singapore, 2017.

[2] A.G. Fane, A grand challenge for membrane desalination: More water, less carbon, Desalination 426 (2018) 155-163.

[3] M. Kostoglou, A.J. Karabelas, Dynamic operation of flat sheet desalination-membrane elements: A comprehensive model accounting for organic fouling, Comput. Chem. Eng. 93 (2016) 1–12.

[4] A.J. Karabelas, M. Kostoglou, C.P. Koutsou, Modeling of spiral wound membrane desalination modules and plants - review and research priorities, Desalination 356 (2015) 165-186.

[5] J. Johnson, M. Busch, Engineering aspects of reverse osmosis module design, Desalin. Water Treat. 15 (2010) 236-248.

[6] M. Kostoglou, A.J. Karabelas, Comprehensive simulation of flat-sheet membrane element performance in steady state desalination, Desalination 316 (2013) 91-102.

[7] E.M.V. Hoek, J. Allred, T. Knoell, B.-H. Jeong, Modeling the effects of fouling on full-scale reverse osmosis process, J. Membr. Sci. 314 (2008) 33-49.

[8] A.J. Karabelas, Key issues for improving the design and operation of membrane modules for desalination plants, Desalin. Water Treat. 52 (2014) 1820-1832.

[9] A.J. Karabelas, C.P. Koutsou, M. Kostoglou, The effect of spiral wound membrane element design characteristics on its performance in steady state desalination — A parametric study, Desalination 332 (2014) 76-90.

[10] C. P. Koutsou, M. Kostoglou, A.J. Karabelas, Membrane desalination under constant water recovery - The effect of module design parameters on system performance, Sep. Purif. Technol. 147 (2015) 90-113.

[11] A. Ghobeity, A. Mitsos, Optimal time-dependent operation of seawater reverse osmosis. Desalination 263 (2010) 76–88.

[12] C. M. Williams, A. Ghobeity, A.J. Pak, A. Mitsos, Simultaneous optimization of size and short-term operation for an RO plant. Desalination 301 (2012) 42–52

[13] M. Johannink, K. Masilamani, A. Mhamdi, S. Roller, W. Marquardt, Predictive pressure drop models for membrane channels with non-woven and woven spacers, Desalination 376 (2015) 41–54.

[14] Y. Roy, M.H. Sharqawy, J.H. Lienhard, Modeling of flatsheet and spiral-wound nanofiltration configurations and its application in seawater nanofiltration. J. Membr. Sci. 493 (2015) 630-642.

[15] M. Kostoglou, A.J. Karabelas, A mathematical study of the evolution of fouling and operating parameters throughout membrane sheets comprising spiral wound modules, Chem. Eng. J. 187 (2012) 222–231.

[16] A.J. Karabelas, D.C. Sioutopoulos, Toward improvement of methods for predicting fouling of desalination membranes - The effect of permeate flux on specific fouling resistance, Desalination 343 (2014) 97-105.

[17] A.J. Karabelas, D.C. Sioutopoulos, New insights into organic gel fouling of reverse osmosis desalination membranes, Desalination 368 (2015) 114-126.

[18] C.P. Koutsou, S.G. Yiantsios, A.J. Karabelas, Direct numerical simulation of flow in spacer-filled channels: effect of spacer geometrical characteristics, J. Membr. Sci. 29 (2007) 53-69.

[19] C.P. Koutsou, S.G. Yiantsios, A.J. Karabelas, A numerical and experimental study of mass transfer in spacer-filled channels: Effects of spacer geometrical characteristics and Schmidt number, J. Membr. Sci. 326 (2009) 234-251.

[20] E.M.V. Hoek, M. Elimelech, Cake-enhanced concentration polarization: anew fouling mechanism for salt rejecting membranes. Environ. Eng. Sci. 37 (2003) 5581–5588.

[21] J.W. Wang, D.S. Dlamini, A.K. Mishra, M.T.M. Pendergast, M.C.Y. Wong, B.B. Mamba, V. Freger, A.R.D. Verliefde, E.M.V. Hoek, A critical review of transport through osmotic membranes J. Membr. Sci. 454 (2014) 516–537.

[22] P. Xu, C. Bellona, J.E. Drewes, Fouling of nanofiltration and reverse osmosis membranes during municipal wastewater reclamation: Membrane autopsy results from pilot-scale investigations, J. Membr. Sci. 353 (2010) 111–121.

[23] C.P. Koutsou, A.J. Karabelas, M. Kostoglou, Fluid dynamics and mass transfer in spacer-filled membrane channels – Effect of uniform channel-gap reduction due to fouling, Fluids 3/1 (2018) 12. https://doi.org/10.3390/fluids3010012.